ISSN 1009－3095 Journal of Zhejiang University SCIENCE V. 3, No. 4, P. 395－400, Sep. －Oct., 2002
http://www.periodicals.com.cn; http://www.zju.edu.cn/English
http://www.zjupress.com; http://lib.zju.edu.cn/eindex.htm; jzu_s@mail.hz.zj.cn

Numerical investigation of cavitating flow behind the cone of a poppet valve in water hydraulic system*

GAO Hong（高 红），FU Xin（傅 新），YANG Hua-yong（杨华勇）
(*State Key Laboratory of Fluid Power Transmission and Control, Zhejiang University, Hangzhou 310027, China*)
TSUKIJI Tetsuhiro
(*Depatment of mechanical engineering, Sophia University, Tokyo, Japan*)

Received July 9, 2001; revision accepted Sep. 5, 2001

Abstract: Computational Fluid Dynamics (CFD) simulations of cavitating flow through water hydraulic poppet valves were performed using advanced RNG k-epsilon turbulence model. The flow was turbulent, incompressible and unsteady, for Reynolds numbers greater than 43 000. The working fluid was water, and the structure of the valve was simplified as a two dimensional axisymmetric geometrical model. Flow field visualization was numerically achieved. The effects of inlet velocity, outlet pressure, opening size as well as poppet angle on cavitation intensity in the poppet valve were numerically investigated. Experimental flow visualization was conducted to capture cavitation images near the orifice in the poppet valve with 30° poppet angle using high speed video camera. The binary cavitating flow field distribution obtained from digital processing of the original cavitation image showed a good agreement with the numerical result.

Key words: Water, Hydraulic poppet valve, Cavitating flow field, Numerical simulation
Document code: A **CLC number:** TH137

INTRODUCTION

With increasing speed and pressure in fluid power transmission system, noise pollution and vibration hazards often occur. As a basic component of the system, a valve may frequently be a source of noise and vibration, of which cavitation is the serious problem. Especially in the water hydraulic system, as the vaporization pressure of the water is much higher than that of the oil, cavitation phenomenon becomes an important factor in the design of components. In addition, cavitation always causes surface erosion, fluid contamination, blockages and reduced volumetric efficiency. So study on cavitating flow in valves is absolutely necessary.

Much experimental research had been published on the flow characteristics of throttle valves, poppet valves and others in many literature, regarding the relationship between cavitation and discharge, and thrust force and pressure distributions in the valves (Inaguma et al., 1988, Oshima, 1989), but the results are still rather limited in accuracy and scope. Aoyama et al. (1988) published results of experimental work on the unsteady cavitation performance in the convergent flow of an oil hydraulic poppet valve. However, experiments were carried out only under two kinds of flow conditions. Variations of critical cavitation number with various rates of pressure change in a valve were experimentally studied. Johnston et al. (1991) conducted experimental investigation of flow and force characteristics of hydraulic poppet and disc valves under steady flow, non-cavitating condition, for Reynolds numbers greater than 2500. With reference to visualized flow patterns, measured flow coefficients and force characteristics showed marked differences depending on valve geometry and opening. Tsukiji et al. (1995) investigated the flow pattern in a poppet valve and the vibration of the poppet by means of both numerical and experimental flow visualizations. Using a discrete vortex method the annular axisymmetric jet flow was numerically visualized. The flow pattern near the orifice with cavitation and

* Project supported by the National Natural Science Foundation of China (No. 59835160) and Scientific Research Foundation for Returned Overseas Chinese Scholars, State Education Ministry of China (No. 50175097)

vibration of the poppet were experimentally observed employing two industrial fiberscopes.

By the advent of Computational Fluid Dynamics (CFD), many numerical simulations of flow fields inside the valves were investigated. Vaughan et al. (1992)' s simulation of flow through poppet valves, and results yielded experimental flow patterns in good qualitative agreement with visualized flow patterns. However, error in the prediction of jet separation and reattachment resulted in quantitative inaccuracies. Ueno et al. (1994) investigated experimentally and numerically the oil flow in a pressure control valve under the assumption of non-cavitating condition, and concluded that the main noise of the testing valves is generated from cavitation; and that the noise was influenced by the valve configuration. Henrik L. S (1999) described experimental and CFD analyses of the internal flow characteristics and flow force in a conical seat valve in a specific range of 500 to 4600 in Re. However, the various and sometimes complex valve geometries, their results were not always correct at high Reynolds numbers. Thus continuing investigation into the performance of valves under cavitating conditions is absolutely necessary.

Using FLUENT's multiphase modeling, the inception of cavitation in a water hydraulic poppet valve is predicted. The effect of inlet velocity, outlet pressure, opening size and poppet angle on the cavitation intensity are simulated and compared. Experimental flow visualization was conducted to capture cavitation images near the orifice in the poppet valve with 30° poppet angle. The simulation results compared well with experimental results.

SIMULATION OF POPPET VALVE

Mathematical model

In view of the axisymmetric jet of the poppet valve, the computational domain is simplified to be two-dimensional axisymmetric. The fluid is assumed viscid and incompressible. The continuity equation and momentum conservation equation are given by

$$\frac{\partial U_i}{\partial x_i} = 0 \quad (1)$$

and

$$\frac{\partial U_i}{\partial t} + U_j \frac{\partial U_i}{\partial x_j} = -\frac{1}{\rho}\frac{\partial P}{\partial x_i} + \nu \frac{\partial^2 U_i}{\partial x_j \partial x_j} + \frac{1}{\rho}\frac{\partial(-\rho \overline{u_i' u_j'})}{\partial x_j} \quad (2)$$

where U_i and U_j are the mean velocity components; u_i' and u_j' are the instantaneous velocity components; P is mean pressure; ρ is fluid density.

The RNG $k-\varepsilon$ turbulence model is derived from the instantaneous Navier-Stokes equations, using a mathematical technique called "renormalization group" (RNG) method. Transport equations for the RNG $k-\varepsilon$ model are similar in form to the standard $k-\varepsilon$ model:

$$\rho \frac{Dk}{Dt} = \frac{\partial}{\partial x_i}\left(\alpha_k \rho C_\mu \frac{k^2}{\varepsilon}\frac{\partial k}{\partial x_i}\right) - \rho \overline{u_i' u_j'} \frac{\partial U_j}{\partial x_i} - \rho\varepsilon \quad (3)$$

$$\rho \frac{D\varepsilon}{Dt} = \frac{\partial}{\partial x_i}\left(\alpha_\varepsilon \rho C_\mu \frac{k^2}{\varepsilon}\frac{\partial \varepsilon}{\partial x_i}\right) - C_{1\varepsilon}\frac{\varepsilon}{k}\rho \overline{u_i' u_j'} \frac{\partial U_j}{\partial x_i} - C_{2\varepsilon}\rho \frac{\varepsilon^2}{k} - R \quad (4)$$

where k is turbulent kinetic energy; ε is dissipation rate; C_μ, $C_{1\varepsilon}$ and $C_{2\varepsilon}$ are coefficients in the turbulence model; α_k and α_ε are the inverse effective Prandtl number for k and ε, respectively.

The term R in the ε equation is

$$R = \frac{C_\mu \rho \eta^3 (1-\eta/\eta_0)}{1+\beta\eta^3}\frac{\varepsilon^2}{k} \quad (5)$$

where $C_\mu = 0.0845$, $\eta = Sk/\varepsilon$, $\eta_0 = 4.38$, $\beta = 0.012$.

Accounting for the effects of swirl or rotation, the turbulent viscosity is

$$\mu_t = \mu_{t0} f\left(\alpha_s, \Omega, \frac{k}{\varepsilon}\right) \quad (6)$$

where Ω is swirl number; α_s is swirl constant. $\alpha_s = 0.05$, and the model constants: $C_{1\varepsilon} = 1.42$, $C_{2\varepsilon} = 1.68$.

Grid generation and boundary condition

The structure of the valve is simplified as a two dimensional axisymmetric geometrical model shown in Fig. 1, where z is valve opening, α is half angle of poppet cone. The topology and the grid of the fluid domain are created in an advanced grid preprocessor gambit. In order to enable the features of the flow field to be well resolved, the solution-adaptive grid feature of Fluent is used in refining the original grid based on the geometry, boundary and numerical solution data on the volume fraction gradient of the water vapor. The adaptive final grids are presented in Fig. 2. The bound aries of the valve are specified as velocity inlet, pressure outlet and wall boundary. The wall is assumed as adiabatic, and therefore no heat transfer between the fluid zone and the solid zone is considered. The initial conditions are assumed respectively as flow rate varied from 1 m/s to 10 m/s at all nodes in the calculation fields. The fluid is water with $\rho = 998.2\ kg/m^3$, $\mu = 0.001003\ kg/m \cdot s$.

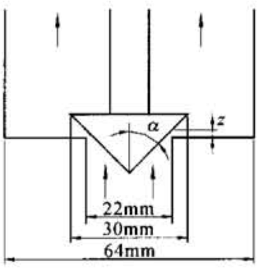

Fig. 1 Schematic diagram of poppet valve

Fig. 2 Solution-adaptive gird of the fluid domain

COMPARISON OF COMPUTATIONAL AND EXPERIMENTAL RESULTS

Cavitating flow visualization in 30° poppet valve was performed using high speed video camera. Fig. 3 shows the binary image of cavitation cloud with the experimental conditions of valve opening $z = 2$ mm, outlet pressure $P_o = 0.1$MPa and inlet velocity $V_i = 5$ m/s. Fig. 3 (a)

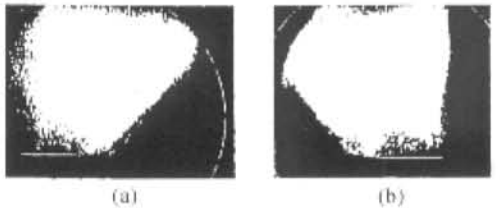

Fig. 3 Binary image of cavitation cloud
(a) side view; (b) front view

and Fig. 3(b) show the side view and front view respectively visualized from different direction. The calculation yielded contours of the volume fraction of water vapor shown in Fig. 4. It was found that cavitation occurred along the poppet surface and covered up the poppet near the orifice. When the local minimum pressure falls to or below the vapor pressure, cavitation occurs and vapor is formed near the orifice of the poppet valve. The calculated region of the high volume fraction of water vapor almost coincided with the experimental region of the cavitation by flow visualization.

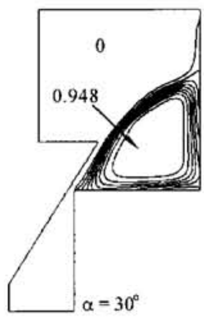

Fig. 4 Contours of volume fractin of water vapor
$z = 2$ mm, $V_i = 5$ m/s, $P_o = 0.1$ MPa

EFFECT OF PARAMETERS ON CAVITATION

A series of cavitating flow simulations were performed with poppet valve over a range of different parameters. The numerically obtained contours of the volume fraction of water vapor showed cavitation inception distribution in the valves. The details of some representative simulation results are described below.

The velocity vector of the fluid and velocity magnitude contour are shown in Fig. 5 (a) and Fig. 5 (b) with $z = 2$ mm and $V_i = 3$ m/s. Clearly there is a recirculation zone near the

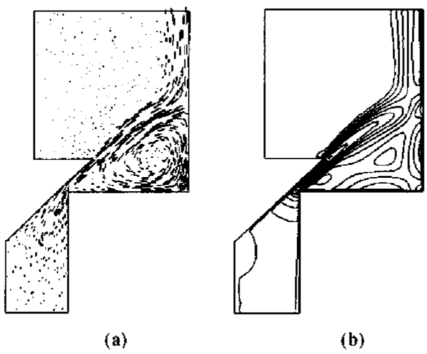

Fig. 5 Velocity vector and magnitude contour
$\alpha = 45°$, $z = 2$ mm, $V_i = 3$ m/s, $P_o = 0.1$ MPa
(a) velocity vector; (b) velocity magnitude contour

orifice region and the recirculation causes formation of the low pressure zone, then possible cavitation. Fig. 6 (a) shows the simulated contours of the volume fraction of water vapor with 45° poppet valve for $V_i = 3$ m/s and 7 m/s, respectively. Here it can be observed that the inlet velocity considerably affects the cavitation intensity. The cavitation inception area was found to be enlarged with increasing inlet velocity and the corresponding volume fraction of water vapor also increased. Fig. 7 shows the effect of inlet velocity on the maximum volume fraction of water vapor, plotted for 45° poppet valve with $z = 2$ mm and $P_o = 0.1$ MPa. As it appears, the maximum volume fraction of water vapor increases with increasing inlet velocity.

Simulations were also performed on 45° poppet valve over a range of outlet pressure from 0.1 MPa to 0.45 MPa. The simulated contours of the volume fraction of water vapor are presented in Fig. 6 (b) with $z = 2$ mm and $V_i = 5$ m/s for $P_o = 0.1$ MPa and $P_o = 0.2$ MPa, respectively. With increase of outlet pressure, the cavitation inception area and the corresponding volume fraction of water vapor are reduced. Fig. 8 shows the maximum volume fraction of water vapor distribution. Obviously the increase of outlet pressure is effective in suppressing cavitation inception.

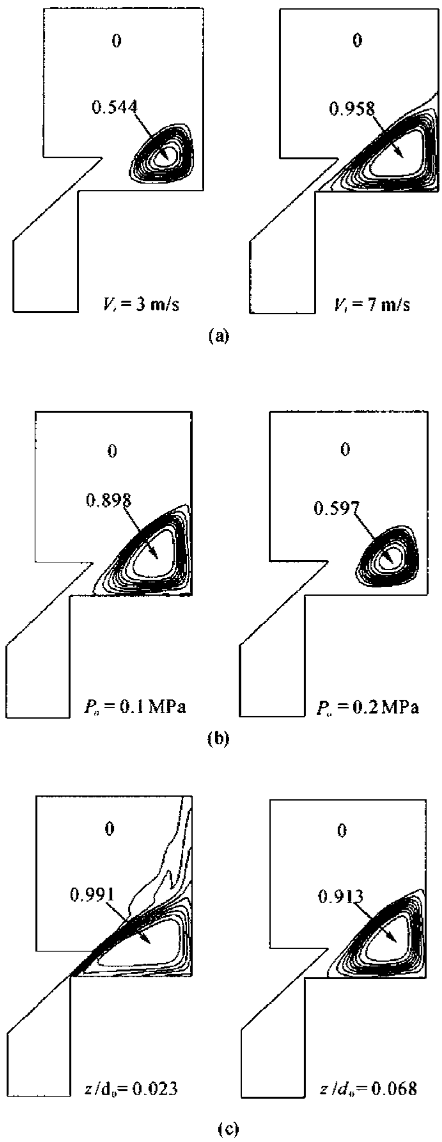

Fig. 6 Contours of volume fractin of water vapor
(a) $\alpha = 45°$, $z = 2$mm, $P_o = 0.1$MPa; (b) $\alpha = 45°$, $z = 2$mm, $V_i = 5$m/s; (c) $\alpha = 45°$, $V_i = 5$m/s, $P_o = 0.1$MPa

The effect of valve opening size was also simulated on 45° poppet valve with a wide range of opening size, from 0.1 mm to 4 mm. Fig. 6 (c) shows the simulated contours of the volume fraction of water vapor for $z = 0.5$ mm ($z/d_0 = 0.023$) and $z = 1.5$ mm ($z/d_0 = 0.068$) with equal inlet velocity and outlet pressure.

Fig. 9 shows the maximum volume fraction of water vapor distribution versus relative valve opening, z/d_0. It is apparent that valve opening has a strong effect on cavitation intensity. At $z/d_0 = 0.023$ ($z = 0.5$ mm), cavitation almost distributes over the entire orifice outlet region and the maximum volume fraction of water vapor reaches 0.991. For $z/d_0 > 0.023$, cavitation inception area and the corresponding volume fraction of water vapor decrease with increasing valve opening.

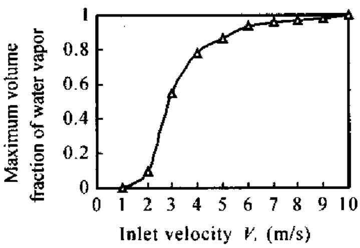

Fig. 7 Effect of inlet velocity on cavitation
$\alpha = 45°$, $z = 2$ mm, $P_o = 0.1$ MPa

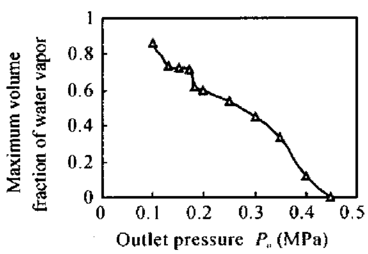

Fig. 8 Effect of outlet pressure on cavitation
$\alpha = 45°$, $z = 2$ mm, $V_i = 5$ m/s

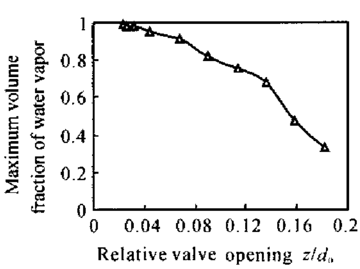

Fig. 9 Effect of relative valve opening on cavitation
$\alpha = 45°$, $V_i = 5$ mm, $P_o = 0.1$ MPa

Cavitating flow in poppet valve with different poppet angle varying from 30° to 70° was simulated in order to investigate the effect of poppet angle. Fig. 4 and Fig. 6 (b) show the contours of the volume fraction of water vapor for poppet angle of 30° and 45° with equal valve opening and boundary condition. Fig. 10 shows the maximum volume fraction of water vapor distribution versus poppet angle. It is clear that the cavitation inception area and the volume fraction of water vapor reduce as the poppet angle increases from 30° to 70°. The maximum volume fraction of water vapor is high for small α and reduces at higher α. For $\alpha = 30°$, the local high value area covers most of the center area behind cone of the poppet valve(Fig. 4). For $\alpha = 55°$, cavitation inception area and the volume fraction of water vapor drop sharply.

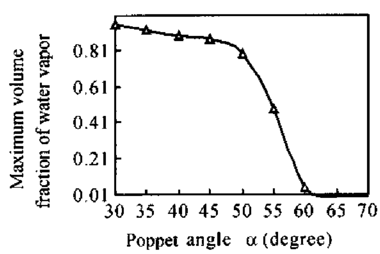

Fig. 10 Effect of poppet angle on cavitation
$V_i = 5$ m/s, $z = 2$ mm, $P_o = 0.1$ MPa

CONCLUSIONS

1. The experimentally visualized cavitation region almost coincided with the numerically predicted water vapor region using RNG k-ε turbulence model, which means that the cavitation region in the poppet valve can be accurately predicted using RNG k-ε turbulence model and the simulation is valid.

2. Recirculation is an important feature of the flow through poppet valves. The cavitating flow characteristics are more sensitive to the intense recirculation zone in the orifice region than to the recirculation occuring downstream of the valve.

3. The numerically predicted contours of the volume fraction of water vapor distribution indicate the cavitation occurs primarily behind the orifice and the corner of conical valve seat.

4. The flow velocity and geometry changes.

For instance, the poppet angle and opening size of the poppet valve can affect significantly the intensity of the cavitation. The increase of the outlet pressure could suppress effectively the inception of the cavitation.

5. The cavitating flow field has great effect on flow energy loss and vibration noise. The analyses in this paper is helpful for further water hydraulic poppet valve structure design for energy saving and noise reduction.

References

Aoyama, Y., Matsuoka, Y., Yamamoto, M., et al., 1988. The cavitation performance of an oil hydraulic poppet valve. *In*: Transactions of the Japan Society of Mechanical Engineers, Part B, 54 (503), p.1710 – 1715.

Henrik L. Sørensen, 1999. Experimental and numerical analysis of flow force compensation methods for hydraulic seat valve. *In*: The Sixth Scandinavian International Conference on Fluid Power Tampere, Finland, p. 471 – 482.

Inaguma, Y., Hibi, A., 1988. A study on cavitation in two-stage hydraulic restrictors. *J. Jpn. Hydro. Pneum. Soc.*, **9** (7): 572(in Japanese).

Johnston, D. N., Edge, K. A., Vaugham., N.D. 1991. Experimental investigation of flow and force characteristics of hydraulic poppet and disc valves. Proc. *Instn. Mech. Engrs*, Part A, p.205: 161.

Lin, J.Z. Zhou Z.X., Wu, T. et al., 2001. Research on disturbance properties of suspensions near the injection area of moving jet. *Journal of Zhejiang University SCIENCE*, **2**(1): 15 – 23.

Oshima, S., 1989. An experimental study on several poppet valves with difference in shape. *In*: JHPS Intern. Sympo. on Fluid Power, Tokyo, p.359.

Tsukiji, T., Yonezawa, Y., Ishii, Y., 1995. Flow in a three-dimensional poppet valve for oil hydraulic power applications. Transactions of the Japan Society of Mechanical Engineers, Part B, 61(583), p.998 – 1004.

Ueno, H., Okajima, A., Tanaka, H., et al., 1994. Noise measurement and numerical simulation of oil flow in pressure control valves. *JSME International Journal* (Series B), **37**(2), 336 – 341.

Vaughan, N. D., Johnston, D. N., Edge, K. A., 1992. Numerical simulation of fluid flow in poppet valves. *Proc. Instn. Mech. Engrs.*, (Part C)206: 119 – 127.